BAUET JOURNAL
Published by
Bangladesh Army University of Engineering & Technology
Journal Homepage: http://journal.bauet.ac.bd

Synthesis and Assessment of Melon Shell Activated Carbon for the Removal of Fe(II) and Mn(II) from Fish Pond Waste Aqua Culture

Abdulrahim IBRAHIM[1], Aliu bdulakeem OLUWADARE[2], Amoo Folahan ADEKOLA[2], Manniru Abdullahi ALI[3]

[1]*Department of Pure and Applied Chemistry, Faculty of Sciences, Kaduna State University, Kaduna, 800283, Nigeria*
[2]*Department of Industrial Chemistry, Faculty of Physical Sciences, University of Ilorin, Ilorin, Nigeria*
[3]*Chemistry Department, School of Sciences, Kano State College of Education and Preliminary Studies, Kano, Nigeria*

Abstract: This article studied a chemically activated carbon prepared from melon shell with KOH as an activating agent. The sample was analyzed by FI-IR, BET, EDX and SEM. Effectiveness and Potentials of the prepared Melon Shell Activated Carbon (MSAC) and the influential factors like adsorbent quantity, initial metals ion concentration, pH, temperature and contact time were as well examined. The process was found to be reliant on all the considered factors, with optimum removal of both metal ions at pH 6.0. The respective adsorption capacity (Langmuir monolayer) for both Fe(II) and Mn(II) ions were found to be 3.148 and 3.706 mg/g respectively. The Langmuir isotherm better described the experimental data. The adsorption kinetics and equilibrium were also better described by Pseudo-second order for Mn(II) ion while none fitted for the uptake of Fe(II) ion. Similarly, thermodynamic parameters such as DG0, DH0 and DS^0 were evaluated. The negative value of ΔG^0 along with the positive value of ΔH^0 and ΔS^0 indicates that the process is spontaneous, endothermic and an irregular increase in the disorderliness at the solid/solution interface of the adsorbent during the process. The results shows that activated carbon prepared from melon shell has potential for the treatment of wastewater from fish farms.

Keywords: *Iron (II); Manganese (II); Fish pond; Activated carbon; Melon shell; waste Aqua Culture.*

Introduction: Globally, significant increase in demand for seafood and fish has made aquaculture industry a fast-growing one. There is a speedy development in aquaculture industry compared to any other part of the animal culture industry. [1]. Generally, different industrial effluents contain heavy metals as pollutants. These heavy metals found their ways into the ground and surface water through Industries like mining, rubber processing, fertilizers, metal plating, and metal finishing, in addition to agriculture [2].The ways and manners with which these heavy metals are released to the ecosystem has become worrisome owing to their harmful nature. Heavy metals pose a danger to man and his environment and are toxic [3]. Iron and manganese are found in groundwater and present in the form of Fe^{2+} and Mn^{2+} ions. [4]. Fe(II) and Mn(II) often occur together in groundwater, but the concentration of manganese is found to be usually much lower than that of iron [5]. The negative effect of iron and manganese are not only aesthetic problems, but also indirect health concerns and economic difficulties [6]. In nature, manganese is the second most abundant metal among heavy metals. Naturally, organisms and plants use Mn(II) ions and Mn(VII) ions of this metal as indispensable micronutrients. Manganese is widely use in ceramics, electrical coils, and dry battery cells as well as many alloys [7]. However, they become toxic at higher concentration. In drinking water, the highest concentration dose of manganese permissible is 0.05 mg/L [8].

Oxidation and aeration combined with filtration or sedimentation are conventionally used to remove Fe and Mn [9, 10]. These methods are time consuming and can be considered not ideal. To remove very minute quantity of pollutants, Fe and Mn inclusive, adsorption is proficient and extensively employed in water treatment applications due to its comparatively simple operation and high efficiency [11]. Adsorption is the most efficient and effective method, which has been used to absorb heavy metals from wastewater especially when using commercial activated carbon [12]. It is widely applied due to its simplicity, cost-effectiveness and environmental friendliness [13].

To develop a new method of economic importance for the effective and efficient removal of Fe(II) and Mn(II) from fishpond wastewater, chemically activated melon shell was engaged as a bio-sorbent. Melon is an extensively spent fruit which belongs to the family of Cucurbitaceae, of which they exist in various species. However, disposal of the shells of these seeds species might be considered as a nutritional and economical loss [14, 15].

The novelty of this study is in the use batch adsorption process and the use of melon shell as a precursor agent for the preparation of the activated carbon composite. Melon shell can be categorized as a byproduct of an agricultural industrial whose commercial and/or industrial application has not been reported; however, they cause severe ecological problems when they undergo oxidation

Article history:
Received 14 May, 2022
Received in revised form 10 June,2022
Accepted 14 October, 2022
Available online 02 November, 2022

Corresponding author details: Abdulrahim Ibrahim
E-mail address: abdulrahim.ibrahim@kasu.edu.ng
Tel: +2348037046497

as a result of their discharged into water bodies and landfills [16 17]. Nevertheless, the information at our disposal has not revealed to us any previous studies on the adsorption of Fe(II) and Mn(II) ions from fishpond effluents via Melon Shell Activated Carbon (MSAC). The possibility of this chemically activated melon shell for efficiently removing Fe(II) and Mn(II) ions from fishponds and other aquaculture effluents therefore needed to be investigated, since many of these farms now face new regulations concerning the quality of water which they are permitted to discharge into natural water bodies.

The present study was carried out in order to investigate the efficiency of melon shell activated carbon in removing excess Fe(II) and Mn(II) ions from fishponds. Equilibrium properties and process kinetics were studied in batch experiments using aqueous solutions of Fe(II) and Mn(II) as well as fishpond effluents.

Materials and Methods

Collection of Melon Shell (MS): The precursor employed for the preparation of the activated carbon in this study was a melon shell (MS), an agro-industrial waste. It was locally sourced from a local market in Share, Ifelodun Local Government Area of Kwara State, Nigeria.

Preparation of Adsorbents: The melon shell (MS) as a precursor material was washed to remove dust and other dirt on it. The washed materials was dried at room temperature, pulverised and sieved through 0.25µm sieve.

The sieved material was kept in the hot air oven at 105ºC for 6 hours. 50 g of dried sample was soaked in 100 ml of 0.1M KOH (1:2 weight by volume) over night and agitated mechanically at reasonable speed for 2 hours. At the end of second hours of stirring, the product was washed with surplus of deionized water to neutrality [18]. The muffle furnace was used to dry washed material at room temperature, ashed at 400 °C for a period of 30 minutes and labeled as MSAC after cooling.

Characterization of Adsorbents: For elemental characterization of the adsorbent, Energy Dispersive X-ray spectrophotometry was used while surface area and pore volume of the adsorbent were determined through nitrogen adsorption techniques (Brunauer-Emmett-Trller, BET). Fourier Transform Infrared (FT-IR) was used to determine the major functional group present in the sample and morphological properties of the adsorbent was studied via scanning electron microscopy (SEM).
The ratio of the weight of the prepared activated carbon to that of the melon shell precursor gives carbon yield, both weights being measured on a dry basis,

$$\text{Yield } (\%) = W_1/W_o \times 100$$

Where W_o is the weight of the melon shell before carbonization and W_1 is the weight of the carbon after being carbonized, washed, and dried.

Method of pH drift was used to determine point of zero charge (pzc). The pH of the 0.01M NaCl was adjusted to a value ranges from 2 and 8 using 0.5M HCl or 0.5M NaOH. 0.1g of adsorbent was added to 20ml of the solution whose pH has been adjusted in a stopped plastic container and equilibrated for 24h. The final pH was determined and plotted against the initial pH. Taken as the pzc is the pH at which initial and final pH intercept [19].

The sample's pH was deduced by placing 1 g of the activated carbon in 20 cm^3 distilled water. Stirred for 6 hours at 250 rpm is the resultant suspension, followed by the filtration of the clear solution and subsequent determination of its pH by the use of Kent digital pH meter (Model 7055).

Collection of Sample of Fish Pond Wastewater : Fish pond wastewater used in this research was collected from a commercial fish farm located in Ilorin, Kwara State. The sample was collected into air tight plastic bottles.

Physico-chemical Characterization of the Fish Pond Wastewater. The physico-chemical properties determined include: Temperature, pH, COD, turbidity, BOD, DO, Fe^{2+} and Mn^{2+}.

Preparation of Adsorbate: Without further purification, reagents used in this study were analytical grade of $FeSO_4 \cdot 6H_2O$ and $MnSO_4 \cdot H_2O$. Stock solutions of 1000 mg/L containing Fe(II) and Mn(II) ions were prepared by dissolving appropriate quantity of their individual salts in different volumetric flask (1000 ml) containing some quantity of deionized water and made up to the mark. Appropriate dilution was done to prepare different working concentrations of 5-50 mg/L from the stock solutions. With the aid of pH meter, drop wise addition of 0.1M NaOH or 0.1M HCl was used to adjust the pH of each solution to values ranges from 2.0–8.0 when required.

Batch Adsorption Experiments: To conduct the adsorption experiments, 25 ml of different concentrations of aqueous solutions containing Fe(II) and Mn(II) were taken into 200 ml transparent plastic bottles which contained accurately weighed quantity of the adsorbent. The bottles were caped and then shaken at 25^0C for a period of 2 hours to attain equilibrium. Filtration method of separation was used to remove the adsorbent and the equilibrium concentration of each metal ion. The concentrations of Fe^{2+} and Mn^{2+} left in the solutions were estimated by taking the difference of the initial and the final metal ion concentrations. Effect of contact time (30-150 min), adsorbent dosage (0.05-0.3 g), initial metals ion concentration (5-50 mg/L), initial solution pH (2-8)

and temperature (25-50^{0}C) on adsorption by MSAC were investigated. A mass balance equation was used to estimate the adsorption capacities as presented below:

$Q_e = VC_o - C_e/ W$

Where Q_e denotes adsorption capacity per gram dry weight of the adsorbent (mg/g) at equilibrium, C_o is the initial metals ion's concentration in the solution (mg/L), C_e is the concentration of metals ion left in the solution (mg/L) at equilibrium, the volume of the solution (L) is denoted as V, and W is the adsorbent's dry weight (g).

Adsorption Isotherms Studies: Adsorption isotherms that better described the experimental data were found to be Freundlich and Langmuir [20, 21]. Mathematical expression for the Langmuir isotherm is given as:

$C_e/q_e = 1/K_{qm} + C_e/q_m$

Where C_e is the adsorbate concentration at equilibrium (mg/L) and q_e is the equilibrium quantity of metal uptake per gram of the adsorbent (mg/g). q_m (mg/g) and K_L (L/ mg) are Langmuir constants associated with adsorption capacity and adsorption rate respectively. The slope and intercept gotten from the Langmuir plot of C_e against C_e/q_e were used to calculate the values of q_m and K_L [22].

Freundlich Adsorption Isotherm: Regarded as an empirical isotherm is the Freundlich isotherm. It designates heterogeneity of the sorbent's surface with interaction between the adsorbed molecules. Freundlich equation in a linearized form is given by:

$\log q_e = (1/n)\log C_e + \log K_f$

Where k_f and n are constants of Freundlich adsorption, associated with adsorption capacity and sorption intensity respectively gotten from the linear plot of $\ln q_e$ against $\ln C_e$ with $\log k_f$ as intercept and 1/n as slope.

Adsorption Kinetics Studies: Pseudo first order and pseudo second order models were used to determine the kinetic mechanism of the adsorption process.

The Pseudo-first Order: As described by the lagergren or pseudo-first order model, the rate of adsorption sites occupation is proportional to the number of available sites [23].The linearized form of the pseudo-first order equation is written as:

$\text{Log}(q_e - q_t) = \log q_e - K_1 t/2.303$

Where the amount of metals ion uptake at time t and equilibrium (mg/g) are designate as q_t and q_e respectively and k_1 is the pseudo-first order adsorption rate constant (min^{-1}).

Pseudo-second order: The theory that biosorption follows a second order mechanism is the one upon which pseudo-second order model is centered. The rate at which available site for adsorption is occupied is proportional to the square of the number of sites available for occupation [24]. The equation can be expressed as given by Ho and McKay [25].

$t/q_t = t/q_e + 1/k_2 qe^2$

Where k_2 is the pseudo-second order rate constant (g/mg/ min). The slope of the plot of t/q_t versus t was used to estimate value of q_e.

Thermodynamics Study: The influence of temperature on the sorption process is shown by thermodynamic study. In general, there are two known types: exothermal and endothermal sorption processes. An increase in sorption which result from rise in temperature shows that the sorption is an endothermal process. However, increasing temperature decreases the sorption which indicates that the sorption is exothermal process. The equation given below could be used to estimate thermodynamic factors like entropy changes (ΔS^0), enthalpy (ΔH^0) and free energy (ΔG^0), for the sorption.

$$\Delta G^O = -RT \ln K_c$$

$$Kc = \frac{C_e}{C_T}$$

Where K_c is the equilibrium constant, C_T is the solid-phase concentration at equilibrium (mg/L) and C_e is the equilibrium concentration in solution (mg/L). ΔS^o ΔG^o and ΔH^o are changes in entropy (J/mol/K), Gibbs free energy (kJ/mol) and enthalpy (kJ/mol) respectively. The gas constant (8.314 J/mol/K) is designated as R and T is the temperature (K). Evaluated from the slope and the intercept of Van't Hoof plots of $\log K_c$ versus 1/T were the values of ΔH^o and ΔS^o [26].

Results and Discussion

From the results obtained, Tables 1 &2 describes the physico-chemical properties and elemental compositions of the Melon Shell Activated Carbon as follows:

Table 1: Physico-chemical Properties of Melon Shell Activated Carbon.

Parameters	**MSAC**
Moisture content (%)	8.83 ± 0.11
Ash content (%)	3.92 ± 0.16
Yield (%)	61.23 ± 0.21
pH	6.7 ± 0.08
Point of zero charge	6.0 ± 0.04
Particle size (mm)	0.25
Surface area (m^2/g)	1719.51
Pore size (cm^3/g)	0.882

Table 2: EDX Analysis and Elemental Composition of Melon Shell Activated Carbon.

Elements (w %)	**MSAC**
C	76.1 ± 1.16
O	22.17 ± 1.13
Al	0.62 ± 0.80
K	0.6 ± 0.24

Effect of Initial Metal Ions Concentration: The adsorption of both metal ions strongly depend on the initial concentration of their respective ions in solution. Presented in fig. 1 is the result of influence of initial concentration on the Fe(II) and Mn(II) ions removal by MSAC, as investigated. Exponential increase in quantity removed was observed for both metal ions as the initial concentration of Fe^{2+} and Mn^{2+} in their respective solution increases. As respective initial concentration of Fe^{2+} and Mn^{2+} increases from 5m g/L to 30m g/L, quantity removed also increases from 0.33 mg/g to 3.25 mg/g and 0.88 mg/g to 3.28 mg/g for Fe^{2+} and Mn^{2+} ion respectively. This may be attributed to the increase in numbers of metal ions competing for unoccupied sites on the adsorbent at higher initial concentration metal ion [27].

As shown in Fig. 1, the adsorption process was fast at the beginning, but it slows down after 30 mg/L for both metal ions. This can be described by the occupation of adsorption site on melon shell activated carbon and the repulsion forces between the similar charges of metal ions (Mn^{2+} and Fe^{2+}) adsorbed on the surface of the MSAC and the respective metal ions (Mn^{2+} and Fe^{2+}) in the bulk solution. These findings are in agreement with the discoveries in literatures [28, 29, 30].

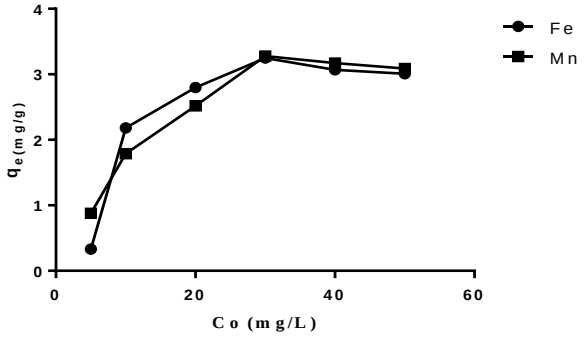

Fig. 1: Effect of initial concentration on adsorption of Fe(II) and Mn(II) onto MSAC.

Effect of Adsorbent Dosage: Shown in Figure 2 is the effect of adsorbent dosage on the adsorption capacity for metal ions (Mn^{2+} and Fe^{2+}) onto MSAC under the following conditions: Co 30mg/L, pH = 4.83 (Mn^{2+}) and 4.45 (Fe^{2+}), temp. 300 K, time 120 minutes. Practically revealed by the adsorption capacity is a contrary trend as presented in figure 2. The adsorption capacity decreased from 9.37 mg/g to 2.35 mg/g and 12.28 mg/g to 1.71 mg/g for $Fe^{2+}$and Mn^{2+} respectively and was best when using 0.05 g of MSAC. This observation (decrease in adsorption capacity) could be attributed to a decline in the operational specific surface area available for metal ions caused by the overlying or clump of adsorption sites, which causes the path length for diffusion of metal ions to increase [31]. As the weight of the adsorbent increased, the aggregation becomes increased significantly. Also, higher MSAC dose which provides more active sites for metal ions (Fe^{2+} and Mn^{2+}) uptake may be responsible for this observation, as a result of which adsorption sites remain unsaturated after adsorption [32]. Therefore, increasing the adsorbent quantity, the amount of metal ions adsorbed onto unit mass of MSAC becomes reduced, consequently a decrease in the q_e value. The result shows that equilibrium metal uptake capacity (q_e) was best when using 0.05 g of MSAC. Hence, the optimum adsorbent dosage chosen was 0.05 g of MSAC. The splitting effect of the concentration gradient between the

adsorbent and adsorbate could also be the one responsible for the observed decrease in the adsorption capacity value (mg metal/g of MSAC) [33].

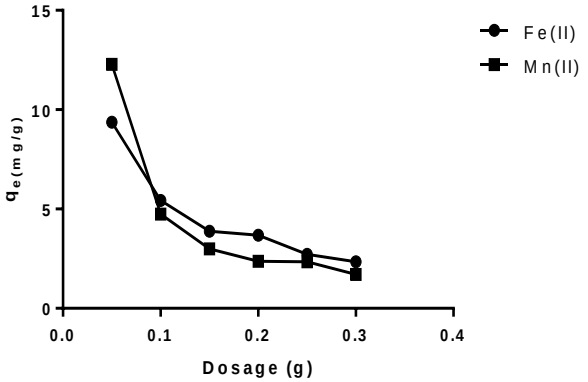

Figure 2: Effect of adsorbent dose on the adsorption of Fe(II) and Mn(II) onto MSAC.

Effect of Contact Time: The effect of contact time on the removal rate of metal ions (Fe^{2+} and Mn^{2+}) by MSAC was investigated at 30 mg/L as the initial concentration of metals ion and the result is as presented in figure 3. It can be seen that increase in contact time increased the quantity of metal ions adsorbed. Fe^{2+} and Mn^{2+} uptake were rapid at the start and progressively go to equilibrium after 90 minutes. The respectful quantity of both Fe^{2+} and Mn^{2+} uptake at equilibrium for initial metal ion concentration of 30 mg/L were found to be 7.48 mg/g and 7.02 mg/g. The initial rapid uptake of the two metal ions could be due to contacts of the metal ions with the surface active sites available for adsorption while gradual adsorption that follows may be attributed to uptake of metal ions into the openings of the adsorbent. Due to the adsorbent large surface area (1719 m^2/g), accumulation of metal ions onto its surface may also be responsible for the observed initial rapid adsorption. Process become slower after the attainment of equilibrium as the active sites is steadily occupied. Furthermore, through intra-particle diffusion which was slower process, the metal ions initially deposited penetrate to the innermost part of the adsorbent. This result agrees with other researcher's observations as stated in the literatures [34, 35, 36].

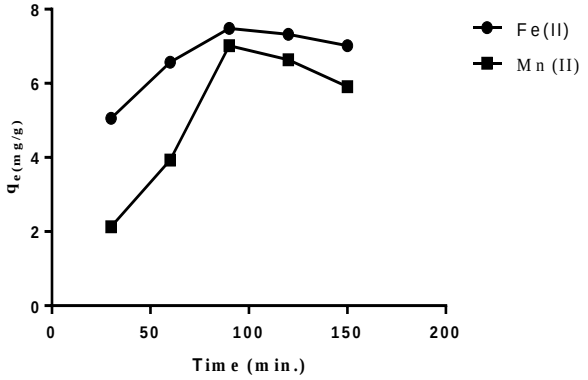

Fig. 3: Effect of contact time on the adsorption of Fe(II) and Mn(II) ions onto MSAC.

Effect of Temperature: The uptake of Mn(II) ions by MSAC rapidly increased when temperature was raised up to 35^oC after which equilibrium was attained while Fe(II) gradually increased as the temperature increases up to 45^0C . These increase in quantity adsorbed might result from two factors; one being the increased rate of pore diffusion and the other being the formation of new active sites on the adsorbent surface. The increase in adsorption site resulting from increased temperature may also signifies likely chemical interactions between the metal ions and the MSAC [37]. Adsorption processes was found to be slightly decreased upon further raised in temperature. Also, the fact that metal ions uptake by MSAC may involve chemisorption in addition to physiosorption and at times involve bond rupture could also be responsible for the observed increase in the quantity of metal ions adsorbed with increased temperature. Increasing temperature also had a notable action on bulge effect within the internal structure of the adsorbent allowing metal cations to infiltrate further thereby increasing the adsorption rate [38]. The process can therefore be said to be endothermic.

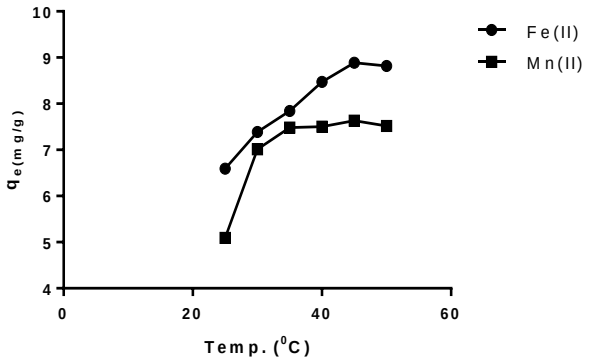

Fig. 4: Effect of temperature (^{0}C) on the adsorption of Fe(II) and Mn(II) ion onto MSAC.

Effect of pH: Another factor which plays a very significant role in the metal ions biosorption is the pH. Hydrogen ions ability to compete with metal ions for the active sites on the surface of biosorbent is directly affected by the differences in initial pH [39]. The consequence of pH on the uptake of Fe(II) and Mn(II) ions onto MSAC was investigated at pH 2–8 and the results are presented in Figure 5. It was observed that as pH increases from 2 to 6, the quantity removed also increases from 0.592 mg/g to 6.42 mg/g for Fe(II) ion and from 2.196 mg/g to 5.753 mg/g for Mn(II) ion. The highest removal (6.42 mg/g for Fe(II) and 5.753 mg/g for Mn(II) ions) was achieved at pH 6. Deprotonation and negative charge of MSAC surface at higher pH may account for the increase in quantity of metal ions removed; consequently, attraction between the positively charged metal and adsorbent occurred, thus causing the absorption onto the biosorbent surface [40, 41]. But biosorption efficiency decreased after attaining the maximum biosorption limit. Formation of soluble hydroxylated complexes of the metal ions and their ionized nature could be responsible for this observation. Also, at higher pH levels, Fe(II) and Mn(II) would be transformed into their hydroxide forms and get precipitated. So, the removal of Fe(II) and Mn(II) could not be established due to adsorption or due to an initial precipitation followed by deposition on the surface of the adsorbent. pH of 6 was used for all subsequent experiments.

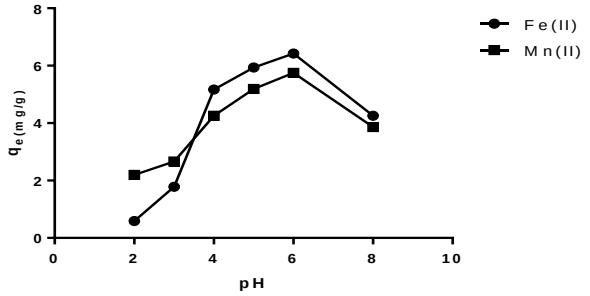

Fig. 5: Effect of pH on the adsorption of Fe(II) and Mn(II) ions onto MSAC.

Adsorption Isotherms

Represented in the figures below are the linear transforms of the adsorption isotherms:

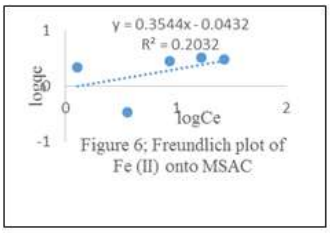

Figure 6; Freundlich plot of Fe (II) onto MSAC

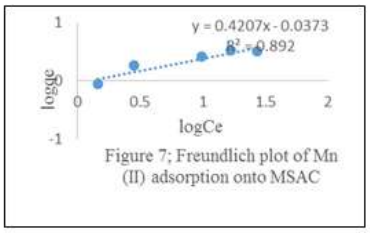

Figure 7; Freundlich plot of Mn (II) adsorption onto MSAC

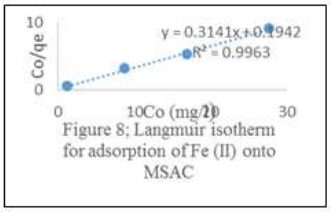

Figure 8; Langmuir isotherm for adsorption of Fe (II) onto MSAC

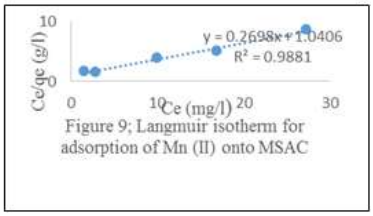

Figure 9; Langmuir isotherm for adsorption of Mn (II) onto MSAC

The freundlich and Langmuir adsorption isotherms constants can be expressed in table 3 and table 4 below:

Table 3: Freundlich Constants.

Metal ions	K_f	1/n	N	R^2
Fe(II)	0.91	0.3544	2.823	0.2032
Mn(II)	0.92	0.4207	2.377	0.8920

Table 4: Langmuir constants.

Metal ions	$1/q_m$	q_m	K_L	R^2
Fe(II)	0.314	3.184	1.617	0.9963
Mn(II)	0.270	3.706	0.259	0.9881

Langmuir and Freundlich equations were the two isotherm equations tested on the obtained results of this study. The equilibrium data obtained from the adsorption of the two metal ions best fitted for Langmuir isotherm due to their high correlation values (R^2) which are 0.996 and 0.9881 for Fe^{2+} and Mn^{2+} respectively This revealed that the uptake of both metal ions by MSAC is physical, homogeneous and monolayer in nature. Also, the values of experimentally determined adsorption capacity (q_e) agreed with the theoretically predicted (q_m) values for Fe^{2+} and Mn^{2+}.

Adsorption deviation from linearity measurement, is the Freundlich constant, n. The adsorption is said to be linear if 'n' value is unity while it is regarded as unfavourable if 'n' value is less than unity. Also, favourable is the adsorption process with n value greater than unity [42]. The values of n at equilibrium were above unity for Fe^{2+} (2.823) and Mn^{2+} (2.377) in the present study, suggesting favourable adsorption.

Adsorption Kinetics: The figures below represents the pseudo-first order and pseudo-second order kinetics for both adsorption of Iron(II) and Manganese(II) unto the melon shell activated carbon.

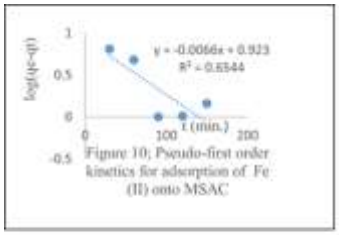

Figure 10; Pseudo-first order kinetics for adsorption of Fe (II) onto MSAC

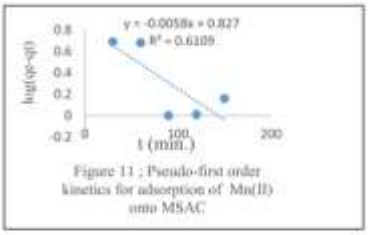

Figure 11 ; Pseudo-first order kinetics for adsorption of Mn(II) onto MSAC

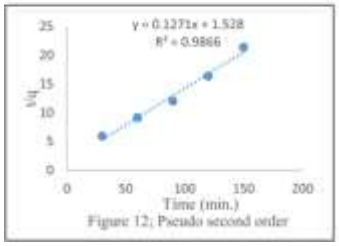

Figure 12; Pseudo second order

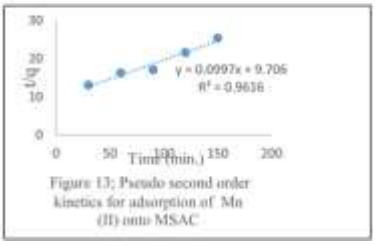

Figure 13; Pseudo second order kinetics for adsorption of Mn (II) onto MSAC

Operation of adsorption as well as its design for Fe(II) and Mn(II) treatment requires a good understanding of batch adsorption kinetics. The chemical or physical features of the adsorbent viz-a-viz its operating conditions are the factors upon which nature of the Mn(II) and Fe(II) adsorption kinetic process depends. Two different models were tested on the kinetic data of Mn(II) and Fe(II) contacts with melon shell activated carbon (MSAC) namely; pseudo-first order and pseudo-second order model. The kinetic data is best described by the pseudo-second order equation. Presented in Figures. 10, 11, 12 and 13 are the adsorption kinetic data for the numerous models. Rate constants and correlation coefficients were estimated from the linear plot of t versus t/q_t (Figures. 10, 11, 12, 13). Correlation coefficients (R^2) values of the data for uptake of both Mn(II) and Fe(II) ions were found to be very high (0.99) as shown in Table 5. From the slope of plot of t versus t/q_t, the rate constant (k) obtained for Mn(II) is 0.013 mg/g min, which is almost the same with that of Fe(II) which is 0.015 mg/g min at equal concentration of 30 mg/L. This suggests that adsorption of both metal ions takes place at almost the same rate. Value of q_e calculated from the pseudo-second order model is in good agreement with the experimental q_e value. This indicates that the kinetic model followed by the sorption process is pseudo-second order [43, 44].

Below were the values of pseudo first order and pseudo second order constants extracted from figures 10 and 11 respectively.

Table 5: Pseudo First Order Constants Extracted from Figures 10 and 11.

Metal ions	$q_{e(cal)}$ (mg/g)	Intercept	R^2	K_1 (g/mg/min.)
Fe(II)	8.375	0.923	0.6544	0.015
Mn(II)	6.714	0.827	0.6109	0.013

Table 6: Pseudo Second Order Constants Extracted From Figures 12 and 13.

Metal ions	$q_{e(cal)}$ (mg/g)	Intercept	R^2	K_2 (g/mg/min.)
Fe(II)	7.87	1.528	0.9866	0.011
Mn(II)	10.03	9.706	0.9616	0.001

Thermodynamic Studies

Table 7: Thermodynamic Parameters of Fe(II) and Mn(II) Adsorption onto MSAC.

Metals	ΔG^o (KJ/ml)	ΔH^o (KJ/mol/K)	ΔS^o (J/mol/K)
Fe	-0.845	+16.812	+49.430
Mn	-1.714	+17.945	+51.019

The thermodynamic for the uptake of Fe(II) and Mn(II) onto MSAC has been investigated in the range of 298-223 K and the influence of temperature on the metal ions uptake under the optimized conditions were studied. Calculated from the slope and intercept respectively were the value of standard enthalpy change (ΔH^o) and standard entropy change (ΔS^o).

It was observed that standard enthalpy change (ΔH^o) for adsorption of Fe^{2+} and Mn^{2+} onto MSAC were found to be +16.812(KJ/mol/K) and +51.019 respectively. This positive value of ΔH^o indicates that the process is endothermic which is buttressed by the increase uptake of Fe(II) and Mn(II) with rise in temperature. In describing the type of adsorption, the magnitude of ΔH^o is very useful. If the size of ΔH^o falls within the range of 2.1–20.9kJ/mol, it signifies a physisorption process, while chemisorption ranges between 80 –200 kJ/mol (Liu and Liu, 2008). From table 6, the value of ΔH^o obtained for Fe(II) ion revealed that the process of metals uptake unto the surface of MSAC is a physical one. The reason why the kinetic data for Fe(II) disagree with the pseudo-second order model (chemisorption model) is explained by the physical adsorption. On the other hand, high value of ΔH^o obtained for Mn(II) (+51.019) is an indication of chemisorption process which may be the reason why the kinetic data for Mn(II) fit the pseudo-second order model (chemisorption model). Also, positive value of ΔS^o implies an increased disorderliness and randomness at the adsorbent-adsobate interface and affinity in the process of adsorption which leads to the increase in entropy and therefore overall positive ΔS^o [45]. Furthermore, the size of ΔS^o reveals whether the mechanism of adsorption reaction is a dissociative or associative one. Conformity of adsorption process to a dissociative mechanism is indicated by the value of ΔS^o being greater than 10 J/molK [46]. The fact that the values of ΔS^o (Table 6) obtained were far greater than $10J/molK^{-1}$ is an indication that the mechanism of Fe(II) and Mn(II) ions adsorption onto MSAC involves a dissociative type.The ΔG^o were calculated at each temperature (298K-223K), and were all found to be negative for both metal ions. These negative values decreased with increased temperature for both metal ions (Table 4). This shows that the process is feasible and that the biosorption process did not gain an external energy which agrees with the reported wok of Vimose et al. and Arias et al [47, 48].

Table 8: Characterization of MSAC Using IR Spectroscopy: FT-IR spectra of melon shell and activated carbon derived from melon shell are illustrated in fig. 14-15 and important peaks extracted from the infrared (IR) spectra of the MSAC are summarized in Table 8.

Raw melon shell	ASSIGNMENT	MSAC	ASSIGNMENT
3414	O-H	3233	O-H
2920	C-H stretching	2936	C-H
_	_	1710.82	C=O
1650	C=O	1603	C=O
1543.61	C=C stretching	1448	CH_2 and CH_3
1435.36	CH_2 and CH_3	1365.70	-C-H bending
1012	C-O strong	1270	C-O

The existence of wide variety of functional groups at the activated carbon surface is well known. These are factors upon which surface properties of activated carbons depend as such, they are essential features of activated carbons. Basic spectra of activated

carbons, especially for determination of types and intensity of their surface functional groups can be provided by the FT-IR spectroscopy. FT-IR spectra of melon shell and activated carbon derived from melon shell are illustrated in fig. 14-15 and important peaks extracted from the infrared (IR) spectra of the MSAC are summarized in Table 8.

Melon shell precursor was found to contain much more bands than activated carbon. The results show that there was disappearance of bands (2660.16 cm^{-1}, 1543.01 cm^{-1}, and 1318.21 cm^{-1}) when spectrum of raw melon shell (precursor) was compared with that of melon shell activated carbon (MSAC), signifying that there were broken of chemical bonds in the course of carbonization process followed by activation [49, 50].

A broad adsorption band at 3000-3600 cm^{-1} is a characteristics of O-H stretching vibrations of hydrogen bonded hydroxyl groups. In the case of precursor, the peak is stronger and has weakened for the activated carbon. The band at 2936.15 cm^{-1} is assigned to asymmetric C-H bond present in alkyl group such as methyl and methylene group. [51]. Stretching adsorption band at 1603.1 cm^{-1} is apportioned to carbonyl C=O found in ester, aldehydes, ketones groups and acetyl derivatives. Adsorption band at 1710.82 cm^{-1} in MSAC spectrum is attributed to C=O of an acid. The band at 1448.02 cm^{-1} can be ascribed to C=H stretching (Saurez-Garcia *et al*., 2002b). The bond at 1270.71cm^{-1} confirms the presence of ester functional group. The intense band at approximately 2920cm^{-1} is assigned to asymmetric C-H stretching, which is reduced in MSAC (2936cm^{-1}), and this indicates that the activation removed a significant amount of hydrogen.

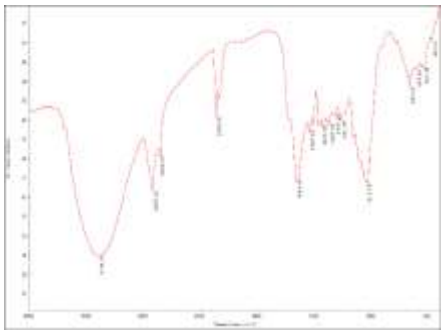

Fig. 14; FTIR Spectrum of Raw Melon Shell.

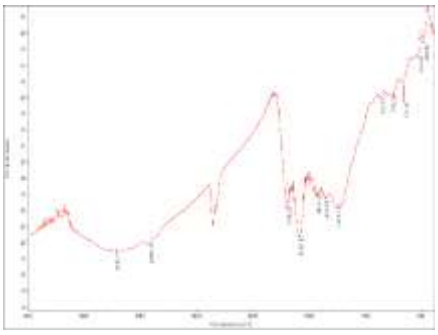

Fig. 15; FTIR Spectrum of MSAC.

Scanning Electron Microscopy :The surface morphology of raw melon shell and melon shell activated carbon (MSAC) were evaluated by Scanning Electron Microscopy (SEM). The resultant SEM micrographs being obtained at 100µm magnifications are as shown in figures 16 and 17. The SEM images shows rough surface area of the carbon which is generally believed to be a good prerequisite for the adsorptive properties. It has been observed that factors like initial structure of the carbon precursor and inorganic impurities influence pore structure development [52].

The surfaces showed particle grains and fibrous like structure (fig. 16, 17). It is obvious that MSAC has considerable numbers of heterogeneous layer of pores where there is a good possibility for metal ions to be adsorbed.

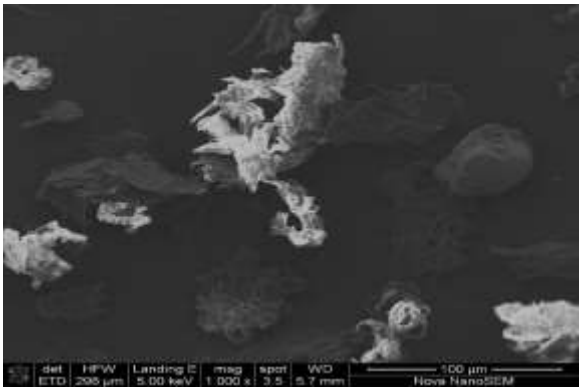

Fig. 16: SEM Micrograph of Raw MS at 100µm.

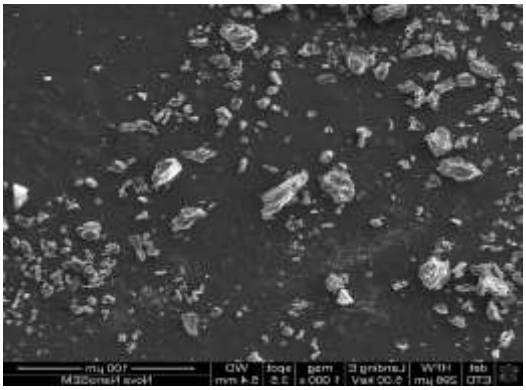

Fig. 17: SEM Micrograph of MSAC at 100µm.

Table 9: Result of Batch Optimization Conditions for the Removal of Mn and Fe Ions from Fishpond Wastewater.

S/N	Properties	Before	After
1	Temperature (^{0}C)	28 ± 0.13	27.80 ± 0.200
2	pH	7.4 ± 0.06	7.15 ± 0.070
3	Conductivity (µs/cm)	404 ± 0.12	174 ± 0.700
4	Turbidity (NTU)	37.84 ± 0.05	6.32 ± 0.030
5	Fe^{2+} (mg/L)	1.40 ± 0.01	0.20 ± 0.003
6	Mn^{2+} (mg/L)	0.11 ± 0.03	0.02 ±0.001

The results are shown in table 9. It is interesting to note that concentration of Mn (II) reduced from 0.11 ± 0.03 mg/L to 0.02 ±0.001 mg/L and that of Fe(II) from 1.40 ± 0.01 mg/L to 0.20 ± 0.003 mg/L after a contact time of 1 hour 30 minutes with adsorbent dose of 0.05 g.

Conclusion: This article studied synthesized activated carbon prepared from melon shell and evaluates its effectiveness for the removal of Fe(II) and Mn(II)ions from fishpond wastewater by adsorption process. It is obvious that initial metal ion concentration, contact time, adsorbent dose, temperature and pH had an outstanding influence on the metal ions uptake by the adsorbent. The study shows that Melon Shell Activated Carbon (MSAC) can be successfully used as an effective and low cost adsorbent for the removal of Fe(II) and Mn(II) ions from fish pond wastewater. The adsorption parameters for the Langmuir and Freundlich isotherms were determined and the equilibrium data were best described by Langmuir isotherm model. Moreover, the kinetics of the adsorption process was shown to be better described by a pseudo-second-order model for Mn(II) when compared to pseudo-first-order while none fitted for the uptake of Fe(II) ion. Also the thermodynamic data have shown that the adsorption of Fe(II) and Mn(II) ions unto MSAC composite is a spontaneous and endothermic process by physiosorption. Surface morphology of the sample was also determined using scanning electron microscopy of 100µm and 10µm magnifications and the pores of char-activated by KOH. The surface of raw melon shell showed a fibrous-like structure while that of activated melon shell showed grains-like structure. The elemental analysis of the precursor (melon shell) and melon shell activated carbon shown that carbon and oxygen are the predominant elements which indicates that the samples is carbonaceous material. Fourier Transform Infrared (FT-IR) shows C=O, C=C, C-C and O-H as the major functional group in precursor and Melon shell activated carbon (MSAC). The BET surface area and pore volume of the melon shell activated carbon were 1719 m^2/g and 0.882 cm^3/g respectively.

References:

[1]. R. L Naylor, R. W. Hardy, A. H. Buschman, S. R. Bush, L. Cao, D. H. Klinger, D. C. Little, J. Lubchenco, S. E. Shumway, M. Troell, Review; A 20-year retrospective review of global aquaculture, Nature. Vol 591 (2021). 551-563. https://doi.org/10.1038/s41586-02103308-6.

[2]. B. Southichak, K. Nakano, M. Normura, N. Chibia, O. Nishmura, Pharagmites australis: a novel bio-adsorbent for the removal of heavy metals from aqueous solution. Water Resources (2006); 40, 2295-2302.

[3]. M. Zaynab, R. Al-Yahai, A. Ameen, Y. Sharif, L. Ali, M. Fatima, K. Ali Khan, S. Li, Review; Health and environmental effects of heavy metals, Journal of king Saud University – Science 34 (2022) 101653, https://doi.org/10.1016/j.jksu s.2021.101653.

[4]. J. L. Lin, C. Huang, J. Pan, Y.S. Wang, Fouling mitigation of a dead-end microfiltration by mixing-enhanced preoxidation for Fe and Mn removal from groundwater. Colloids and Surfaces A: A Physicochemical and Engineering Aspects (2013); 419, 87–93.

[5.] R. El Araby, S. Hawash, G. El Diwani, Treatment of iron and manganese in simulated groundwater via ozone technology. Desalination (2009), 249(3):1345–1349

[6]. G.C. Gosh, Md. J.H. Khan, T.K. Chakraborty, S. Zaman, A.H.M.E. Kabir, H. Tanaka, Human health risk assessment of elevated and variable manganese intake with arsenic-safe ground water in jashore, Bangladesh, Scientific Reports Volume 10, Article number: 5206 (2020).

[7]. M. Suguna, N.S. Kumar, V. Subbaiah, Krishnaiah, Removal of divalent manganese from aqueous solution using Tamarindusnindica Fruit Nut Shell, J. of Chem. and Pharm. Research (2010) 2(1), 7-20.

[8]. World Health Organization (WHO). Manganese in Drinking Water, Guidelines for Drinking Water Quality 2011.

[9]. A. Korchef, I. Kerkeni, M.B. Amor, S. Galland, F. Persin, Iron removal from aqueous solution by oxidation, precipitation and ultrafiltration. Desalination and Water Treatment (2009) 9,1−8.

[10]. S.Y. Qin, F. Ma, P. Huang, J.X. Yang, Fe(II) and Mn(II) removal from drilled well water: A case study from a biological treatment unit in Harbin, Desalination (2009) 245, 183−193.

[11]. H. Yan, L. Yang, Z. Yang, H. Yang, A. Li A, Preparation of chitosan/poly (acrylic acid) magnetic composite microspheres and applications in the removal of Copper(II) ions from aqueous Solutions, J. of Hazard Materials (2012) 229, 371−380.

[12] K.S. Obayomi, J.O. Bello, J.S. Nnoruka, A.A. Adediran, P.O. Olajide, Development of low-cost bio-adsorbent from agricultural waste composite for Pb(II) and As(III) sorptionfrom aqueous solution, Cogent Engineering, 6(1), 1687274. https://doi.org/10.1080/23311916.2019.1687274.

[13] H. Karami, Heavy metals removal from water by magnetite nanorods, Chem Eng. Journal (Amsterdam, Neth.), (2019) 209-216. http://dx.doi.org/10.1016/j.cej.2013.01.022.

[14]. A.R.N Raihana, J.M.N. Marikkar, I. Amin, M. Shuhaimi, A review on Food Values of Selected Tropical Fruit's Seeds, Internat. J. of Food properties, volume 18, (2015) – 1ssue 11, pages 2380-2392.

[15]. E. Florez-Lopez, C.D. Grande-Tovar, The potential of selected Agri-Food Loss and Waste to Contribute to a Circular Economy: Application in the Food, Cosmetics and Pharmaceutical Industries, Molecules (2021), 26(2), 515; https://doi.org/10.3390/molecules26020515.

[16]. L. Chen, Y.H. Kang, J.K. Suh, Roasting processed oriental melon (Cucumis melo L. var. makuwa Makino) seed influenced the triglyceride profile and the inhibitory potential against key enzymes relevant for hyperglycemia, Food Research International (2014) 56, 236–242.
[17]. A Verzera, G. Dima, G. Tripodi, C. Condurso, P. Crino, Aroma and sensory quality of honeydew melon fruits (Cucumis melo L.) in relation to different rootstocks, Science Hortic (2014) 169, 118–124.
[18]. J.A. Ahamed, A.K. Riaz, Preparation and characterization of activated carbon from theprosopis Juliflora plant, Asian Journal of Chemistry (2008) 20(3):1702-1706.
[19]. Y. Yang, Y. Chun, G. Sheng, M. Huang, pH dependence of pesticide adsorption by wheat-residue-derived black carbon, Langmuir (2004) 20, 6736-6741.
[20]. K.R. Hall, L.C. Eggleton, A. Acrivos, T.H. Vermeulan, Pore and solid-diffusion kinetics in fixed bed adsorption under constant pattern conditions, Industrial and Engineering Chemistry Fundamentals (1996) 5(2):212–223.
[21]. N.D. Hutson, R.T. Yang, Theoretical basis for the Dubinin Radushkevich (D-R) adsorption isotherm equation. Adsorption (1997) 3,189–195.
[22]. Langmuir I, The adsorption of gases on plane surfaces of glass, mica and platinum, The Journal of the American Chemical Society (1918) 40(9), 1361–1403.
[23]. G. Blazquez, M.A. Martin-Lara, G. Tenorio, C. Calero, Batch biosorption of lead from aqueous solution by olive tree pruning waste: equilibrium, kinetic and thermodynamic study, Chem. Eng. Journal (2011) 168, 170–177.
[24]. G. Mckay, Y.S. Ho, Pseudo-second order model for sorption process, Process Biochemistry (1999) 34, 451–465.
[25]. Y.S Ho, G. McKay, Application of kinetic models to the sorption of Cu(II) onto Peat, Adsorption Sci. Tech. (2002) 20(8):797–815.
[26]. D. Mohan, K.P. Singh, Single and multi-component adsorption of cadmium and zinc using activated carbon derived from bagasse- an agricultural waste, Water Resources (2002) 6, 2304-2318.
[27]. O.S. Ayanda, S.F. Olalekan, A.A. Folahan, J.X. Bhekumusa, Kinetics and equilibrium models for the sorption of tributylin to nZnO, activated carbon and nZnO/activated carbon composite in artificial seawater, Marine Pollution Bulletin (2013) 72, 222–230.
[28]. O.D. Nwako, T.C. Mogbo, Preliminary study on the use of Urea activated melon (*Citrullus colocynthis*) Husk in the adsorption of Cadmium from wastewater, Animal research international (2014) 11(2), 1917-1924.
[29]. J. Mehdi, J.S. Seyed, A. Javad, R. Alimorad, K. Hossein *et al.,* Preparation of activated carbon from walnut shell and its utilization for manufacturing organic-vapour respirator cartridge, Fresenius Environmental Bulletin (2014) 21, 1508-1514.
[30]. F.A. Adeyemi, K.T. Dauda, Efficiency of seed oil (Pentaclethramacrophlla) shell in removal of Nickel(II) ion from aqueous solution, J. of applied chemistry (2014) 7(6):8-15.
[31]. Y. Li, B. Xia, WQ. Zhao, F. Liu, P. Zhang *et al*., Removal of copper ions from aqueous solution by calcium alginate immobilized kaolin, J. of Environmental Sci. (2011) 23, (3), 404–411.
[32]. C. Raji, T.S. Anirudhan, Kinetics of Pb(II) adsorption by polyacrylamide grafted sawdust, Indian J. of Chemical. Tech. (1997) 4, 157–162.
[33]. B.K. Nandi, A. Goswami, A.K. Das, B. Mondal, M.K. Purkait, Kinetic and equilibrium studies on the adsorption of crystal violet dye using kaolin as an adsorbent, Separation and Sci. Tech. (2008) 43, 1382.
[34]. M.R. Sangi, A. Shahmoradi, J. Zolgharnein, G.H. Azimi, M. Ghorbandoost, Removal and recovery of heavy metals from aqueous solution using ulmus carpinifolia and Fraxinus excelsior tree leaves, Journal of Hazard Materials (2008) 155, 513-522.
[35]. A.A. Iyinbor, F.A. Adekola, G.A. Olatunji, Kinetics, Isotherms and Thermodynamic modeling of liquid phase adsorption of Rhodamine B dye onto *Raphia hookerie* fruit epicarp, J. of Water Resources and Industry (2016) 15, 14-27.
[36]. A.A. Jimoh, G.B. Adebayo, K.O.I. Otun, A.T.I Ajiboye, A.T.I Bale *et al*., Sorption study of Cd(II) from aqueous solution using activated carbon prepared from Vitellaria paradoxa shell, Journal of Bioremediation and Biodegradation (2015) 6(3), 1-10.
[37]. A.S. Ekop, N.O. Eddy, Thermodynamic study on the adsorption of Pb(II) and Zn(II) from aqueous solution by human hair, E-Journal of chemistry (2010) 6 (4):1029-1034.
[38]. T.O Jimoh TO, Yisa J, Ajai AI, Musa A. Kinetics and thermodynamics studies of the biosorption of Pb(II) , Cd(II) and Zn(II) ions from aqueous solutions by sweet orange (Citrus sinensis Seeds), Internat. J. of Modern Chemistry (2013) 4(1), 19-37.
[39]. V.C. Srivastava, M.M. Swamy, I.D. Mall, B. Prasad, I.M. Mishra, Adsorptive removal of phenol by bagasse fly ash and activated carbon: equilibrium, kinetics and thermodynamics, Colloids and Surfaces A: Physicochemical and Engineering Aspects (2006) 272(1-2), 89–104.
[40]. A. Sharma, K.G. Bhattacharyya, Azadirachta indica leaf powder as an effective biosorbent for dyes: a case study with aqueous congo red solutions, Journal of Environmental Management (2006) 71(3), 217–229.
[41]. S.R. Taffarel, J. Rubio, On the removal of Mn^{2+} ions by adsorption onto natural and activated Chilean zeolites, Minerals Engineering (2009) 22, (4), 336–343.
[42]. M. Roulia, A.A. Vassiliadis, Microporous Mesoporous Materials, Carbon (1998) 116, 732-738.
[43]. T.R, Muraleedharan, C. Venkobachar, Mechanism of biosorption of Cu (II) by Ganoderma lucidum, Biotechnology Bioengineering (1990) 35, 320–325.
[44]. D. Park, Y.S. Yun, S.R. Lim, J.M. Park, Kinetic analysis and mathematical modeling of Cr(VI) removal in a different reactor parked with ecklonia biomass, Journal of Microbiology and Biotechnology (2006) 16(2), 1720–1727.
[45]. O.S. Lawal, A.R. Sanni, I.A. Ajayi, O.O. Rabiu, Equilibrium, thermodynamic and kinetic studies for the biosorption of aqueous lead(II) ions onto the seed husk of Calophyllum inophyllum, Journal of Hazard Materials (2010) 177, 829-835.
[46]. Y. Liu, Y.J. Liu, Biosorption isotherms, kinetics and thermodynamics, Separation and Purification Technology (2008) 61, 229–242.
[47]. V. Vimonses, V. Lei, B.J. Chris, V. Chow, C. Saint, Adsorption of Congo red by three Australian Kaolins, Apply Clay Science (2009) 43(3-4), 465-472.
[48]. F. Arias, T.K. Sen, Removal of zinc metal ion (Zn^{2+}) from its aqueous solution by Kaolin Clay mineral: A kinetic and equilibrium study, Revue source colloids and Surface A: Physicochemical and engineering aspects (2009) 348, 100-108.
[49]. M. Jagtoyen, F. Derbyshire, Activated carbon from yellow poplar and white Oak by H_3PO_4 activation, Carbon (1998) 36, 1085-1097.
[50]. F. Saurez-Garcia, A. Martinez-Alonso, J.M.D. Tascon, Pyrolysis of apple pulp: Effective of operation conditions and chemical additives, Journal of Analytical and Applied Pyrolysis (2002) 62, 93-109.
[51] E. Yagmur, M. Ozmark, A. Aktas, A novel method for production of activated carbon from waste tea by chemical activation with microwave energy, Fuel (2008) 87, 3278-3285.

[52]. H. Deng, G. Li, H. Yang, J. Tang, T. Tang, Preparation of activated carbons from cotton stalk by microwave assisted KOH and K_2CO_3 activation, Chemical Engineering Journal (2010) 163, 373-381.